

## **The theoretical and experimental investigations of fixed end beam bending**

E. Khabibulin<sup>1</sup>, A. Sakharov<sup>1</sup>, E. Karulin<sup>2,6</sup>, A. Marchenko<sup>3,4</sup>, D. Sodhi<sup>5</sup>, M. Karulina<sup>2</sup> and P. Chistyakov<sup>1</sup>

<sup>1</sup> Moscow State University, Moscow, Russia

<sup>2</sup>Krylov State Research Centre, St.-Petersburg, Russia

<sup>3</sup>The University Centre in Svalbard, Longyearbyen, Norway

<sup>4</sup>Norwegian University of Science and Technology, Trondheim, Norway

<sup>5</sup> Retired from Cold Region Research Engineering Laboratory, Hanover, NH, USA

<sup>6</sup> State Marine Technical University, St.-Petersburg, Russia

### **ABSTRACT**

The recent results of the fixed end beam failure mechanism in the three-point bending tests are discussed. The fixed end beam model and laboratory tests were investigated by D.Sodhi (1998) as an approach for the breakthrough problem for the floating ice sheet. Full-scale tests with floating fixed-ends beams of natural sea ice were carried out in 2016-2020 in Van-Mijen fiord on Svalbard in the framework of the projects SAMCOT and AOSEC. Pressure load cells were frozen in the beams to measure the clamping force. This method of testing was also useful to determine the flexural and compressive strength of the sea ice depending on its structure, temperature and salinity. The theoretic analysis on the two key problems was provided: a) the crack propagation during bending (elastic behavior), b) post buckling under compression (elastoplastic behavior). Clamping forces obtained from the tests were compared the clamping forces obtained by the numerical simulations. The performed investigation, with the help of rigorous mathematical methods, makes possible to study the formation of cracks in the sea ice sheets, to evaluate the breakthrough loads, and to formulate practical recommendations important for the organizing of ice roads in ice covered regions of Arctic seas.

**KEY WORDS:** 3-point bending, breaking, closing crack, yielding, sea ice.

### **INTRODUCTION**

The development of modern Arctic marine technologies requires new icebreaking and transport vessels, fixed drilling rigs and other special technical facilities for operation in ice conditions. At the same time, correct calculation of ice loads under different scenarios of interaction between ice fields and structures plays the most important role for operational safety assessment. Interactions of this kind are unique in a number of parameters. The area of direct contact, accompanied by ice destruction, with a supporting structure can be tens of square meters, and the speed of ice and structure convergence is also significant (Sanderson, 1988). In such a situation, obtaining empirical data on the failure process patterns at an appropriate spatial and temporal scale becomes time-consuming and expensive. Therefore, the development of appropriate mathematical models of fracture (Dempsey, et al., 1988, Dempsey, 1991, Goldstein and Osipenko, 1983, 1985) and their verification based on the results of field tests and experiments in ice basins is of great importance.

Investigation of failure and bearing capacity of a beam at 3-point constrained bending provides an insight into the processes occurring during punching of ice floe by a concentrated load. Characteristic features of the bending process are the development of root and central cracks, the occurrence of spacing - transverse compressive forces that constrain the deformation process and lead to crack closure, the appearance of areas of compression and ice crushing in these compression areas. The effect of crack closure in the study of the bearing capacity of floating ice plates has been studied by L. Slepyan (L. Slepyan, L. Dempsey, J., 1995).

### A CHARACTERISTIC FEATURE OF FAILURE OF BEAM WITH FIXED ENDS.

The problem of equilibrium of an elastic beam with a notch in cramped three-point bending is the key problem in studying the bearing capacity of a material under the action of distributed or concentrated forces, in particular, when a helicopter lands on an ice cover or a submarine resurfaces in solid ice. Field tests show that, under concentrated loading, the bearing capacity of ice is exhausted at loads greater than the appearance of the first cracks. In order to study the characteristic feature, (D. Sodhi, 1998) proposed to investigate a floating ice plate of considerable size, in which two parallel cuts of equal length are made, forming a beam, the width of the beam being approximately equal to the thickness. During tests the beam is loaded with a concentrated vertical load in the centre, developed by a hydraulic cylinder at a constant stroke rate. In full-scale experiments, multiple failure scenarios were observed.

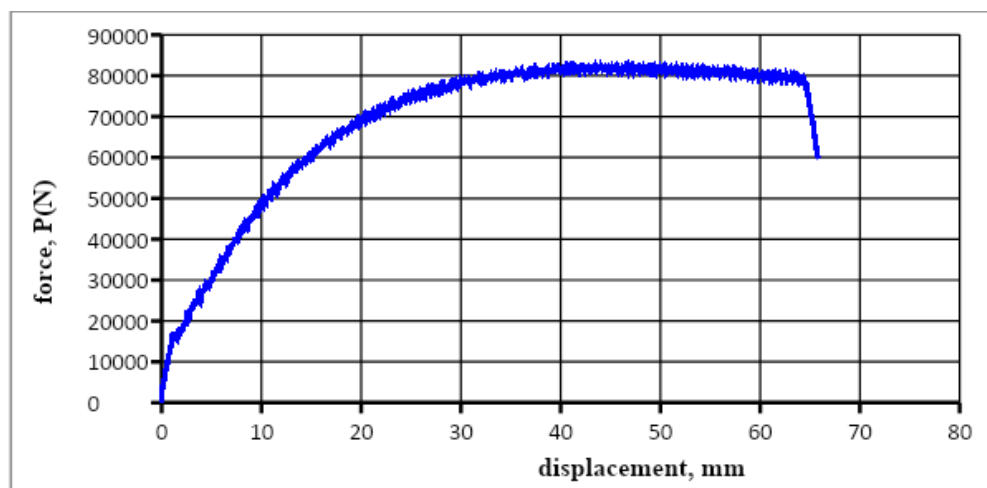


Figure 1. Natural experiment, plot “load vs deflection”.

A typical deformation curve of ice beams with fixed ends in full-scale tests on sea ice is shown in (Fig. 1). The length of the beam was approximately 6 times its height ( $h=0.7\text{m}$ ) and the loading was set by hydraulic cylinder rod stroke at a speed of 2 to 10mm/min. The initiation and development of cracks occurred at loads less than 2 tf, and the exhaustion of the beam carrying capacity at loads over 8 tf. It is possible to observe on the graphic the sequence of the process - linear section of deformation, appearance of central and two cracks at the beam root, and then non-linear section of deformation where the material of the beam shows plastic properties. Thus, a multi-stage deformation pattern is observed in the beam tests. Further balancing of the increasing load is provided by the expansion forces resulting from wedging, which cause the beam to be subjected to predominantly compressive stresses, relative to which the ice is very strong. The most characteristic feature is the constriction of the deformation, resulting in the phenomenon of slowed crack growth followed by the stopping and closing of the crack tip.

In this paper, an attempt is made to describe both deformation stages (both elastic and inelastic) from the unified perspective of fracture mechanics. To describe the elastic stage, linear fracture mechanics (Irwin-Orovann concept, P. Paris formula) is used. For the nonlinear

stage of deformation, a theory based on the J-integral relation to the crack opening in the full-scale fluidity of the material in the singular region is used.

### THE PROBLEM OF THE 3POINT BENDING UNDER CONSTRAINT (ELASTIC STAGE).

A special feature of Sodi beam loading compared to cantilever beam bending is the constriction, the occurrence of longitudinal forces along with bending moment and transverse force. The longitudinal force  $N$  and the bending moment  $M$  arise as a response to kinematic connections, so Castigliano's theorem is effective for calculation.

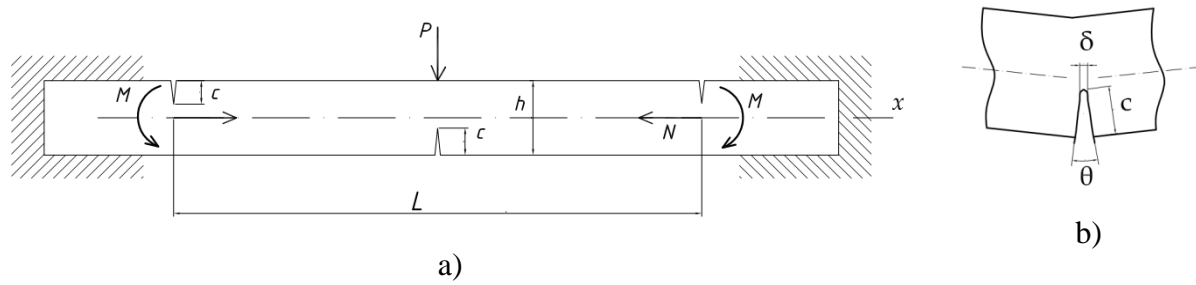


Figure 2. Model of elastic beam

When solving the problem, we assume that the root ( $x=\pm l/2$ ) and central ( $x=0$ ) cracks have the same length and are the cracks of normal separation, i.e. we neglect the influence of transverse force in the embedment on the crack development. In order to compose the kinematic conditions for the coupling of the beam with the singular regions, let us introduce the crack opening  $\delta$  and the rotation of the banks  $\theta$ . We will follow the method of J. Rice, N. Levy (1972) by representing the singular regions as elastic elements, the yielding of which is determined from the solution of the strip-cut problem. Then for each section of the beam we can write:

$$[u(x_c)] = \delta; [w'] = \theta \quad (1)$$

where  $[\ ]$  is the singular discontinuity  $x_c = 0; \pm l/2$ , i.e.  $u; w'$  Following Irwin, let's write down the energy change associated with crack growth

$$G = \frac{dU_c}{dA} \quad (2)$$

where  $dA$  is the change in crack area,  $U_c$  is the fraction of body energy changing during crack

growth when forces remain constant; the fracture toughness is  $G = \frac{K_I^2}{E'}$ ,  $E' = E / (1 - \nu^2)$ ,  $K_I$

is the intensity coefficient at the crack tip,  $E; \nu$  is the Young's modulus and Poisson's ratio. Due to the superposition principle for the intensity coefficient

$$K_I = K_{IM} + K_{IN} = (\sigma_M f_M(\omega) + \sigma_N f_N(\omega)) \sqrt{\pi c} \quad (3)$$

where  $\sigma_M = \frac{6M}{bh^2}$ ,  $\sigma_N = \frac{N}{bh}$  is the reduced stress,  $\omega = c/h$  is the dimensionless crack length parameter,  $f_M(\omega)$ ,  $f_N(\omega)$  is the known gauge functions represented by Lagrange polynomials (formulas 2.11, 2.13; Tada et al, 2000). Due to the assumption of uniformity of crack development the problem is statically determinable, it follows from the equilibrium condition  $M=Pl/8$ .

Let us use the Castiliano theorem and the formula of P. Paris (App. B; Tada et al, 2000) to determine the generalized displacements:

$$\Delta_M = \Delta_{0M} + \Delta_{Mc} = \frac{\partial U_0}{\partial M} + \frac{\partial}{\partial M} \left( \int_0^A G \cdot dA \right)$$

$$\Delta_N = \Delta_{0N} + \Delta_{Nc} = \frac{\partial U_0}{\partial N} + \frac{\partial}{\partial N} \left( \int_0^A G \cdot dA \right)$$

(4)

(5)

where is the  $\Delta_M$ ;  $\Delta_N - M, N$ . Since  $N$  is a reaction, then

$$\Delta_N = u(x_c) + \delta / 2 = 0$$

(6)

The system, due to the symmetry of the problem, will be understood as a 1/4 girder. Let us write down the elastic energy of the system  $U_0$

$$U_0 = \frac{1}{2} \int_0^{l/4} \left( \frac{M^2(x)}{EJ} + \frac{N^2}{EA} \right) \cdot dx = \frac{M^2 l}{Ebh^3} + \frac{N^2 l}{8Ebh}$$

(7)

$$\Delta_{0N} = u(0) = \frac{Nl}{4Ebh} = \frac{\sigma_N l}{4E}$$

Then We find the generalised displacements of the singular regions as:

$$\delta / 2 = \frac{\partial}{\partial N} \left( \int_0^A G \cdot dA \right) = \frac{2\pi h}{E'} \int_0^\omega (\sigma_M f_M(\omega) + \sigma_N f_N(\omega)) f_N(\omega) \omega d\omega$$

(8)

$$\theta / 2 = \frac{\partial}{\partial M} \left( \int_0^A G \cdot dA \right) = \frac{12\pi}{E'} \int_0^\omega (\sigma_M f_M(\omega) + \sigma_N f_N(\omega)) f_M(\omega) \omega d\omega$$

(9)

Since the change in the energy of the body due to the change in the crack area occurs when the forces are constant,  $\sigma_M$ ;  $\sigma_N$  we carry the integral beyond the sign of the integral. Let's

$$J_{ab}(\omega) = \int_0^\omega f_a(\omega) f_b(\omega) \omega d\omega$$

introduce the coefficients of suppleness  $J_{ab}(\omega)$ ,  $a, b = M, N$ , which are calculated through tare functions. From equation (6) we find the unknown value of the reactive force

$$\sigma_N = - \frac{J_{MN}(\omega)}{\zeta / 4 + J_{NN}(\omega)} \sigma_M$$

(10)

$$\zeta = \frac{l}{2\pi(1-\nu^2)h}$$

where is the dimensionless parameter defining the proportion of the beam.

Not only does the crack growth occur due to the appearance of cracks in the beam, but it also forms the condition for its development itself. If we use the force criterion for crack growth

$K_I = K_{IC}$ , condition (3) closes the problem of determining crack growth conditions:

$$\left( f_M(\omega) - \frac{J_{MN}(\omega)}{\zeta/4 + J_{NN}(\omega)} f_N(\omega) \right) \sigma_M \sqrt{\omega} = K_{IC} \quad (11)$$

Also, since  $\sigma_N; \sigma_M$  they have different signs, if there are such proportions  $\zeta$  of the girder and such a crack length, when the multiplier before is  $\sigma_M$  zero. Then at any value of load the girder cannot be split apart by cracks. The phenomenon of crack closure arises. The family curves  $\sigma_N; \sigma_M$   $\sigma_M(\omega_M(\zeta), \zeta) = \min \sigma_M(\omega, \zeta)$ . The stationary value distinguishes two branches of the cracked body states: ( $\omega < \omega_m$ ) the bending branch, where the bending form of equilibrium prevails, and the propagation branch ( $\omega > \omega_m$ ).

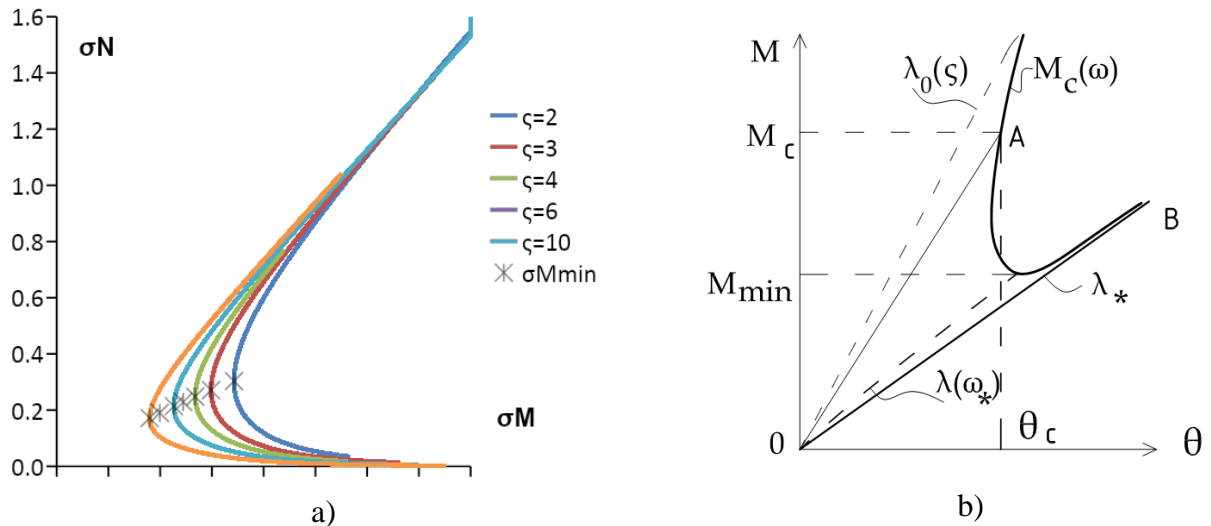


Figure 3. Deformation curves of the strip at different notch lengths

In Fig. 3b. the deformation curves of the strip at different notch lengths up to the limit state are plotted on the plane ( $M; \theta$ )  $M_c(\omega)$ . The straight line  $OB$  is the asymptote for the states of the spacer branch with the yielding  $\lambda_*$ ,  $M_{min} = \min M(\omega)$  - defines the lower boundary of the crack instability.

In order to study the influence of the constraint factor, the bending problem of a beam with an antisymmetrical notch system (fig.2a), fixed against longitudinal displacements, was considered ( $\zeta, \omega$ ) - dimensionless geometric parameters of the problem.

This problem was modelled and solved by the finite element method. During the solution, the intensity coefficient  $K_I$  and the yield strength  $\Delta_P/P$  - the ratio of deflection to load - were determined. To determine  $K_I$ , a numerical J-integral method was used in the ANSYS Mechanical APDL package. The mesh on the modelled beam was created with SOLID186 elements (fig. 4)

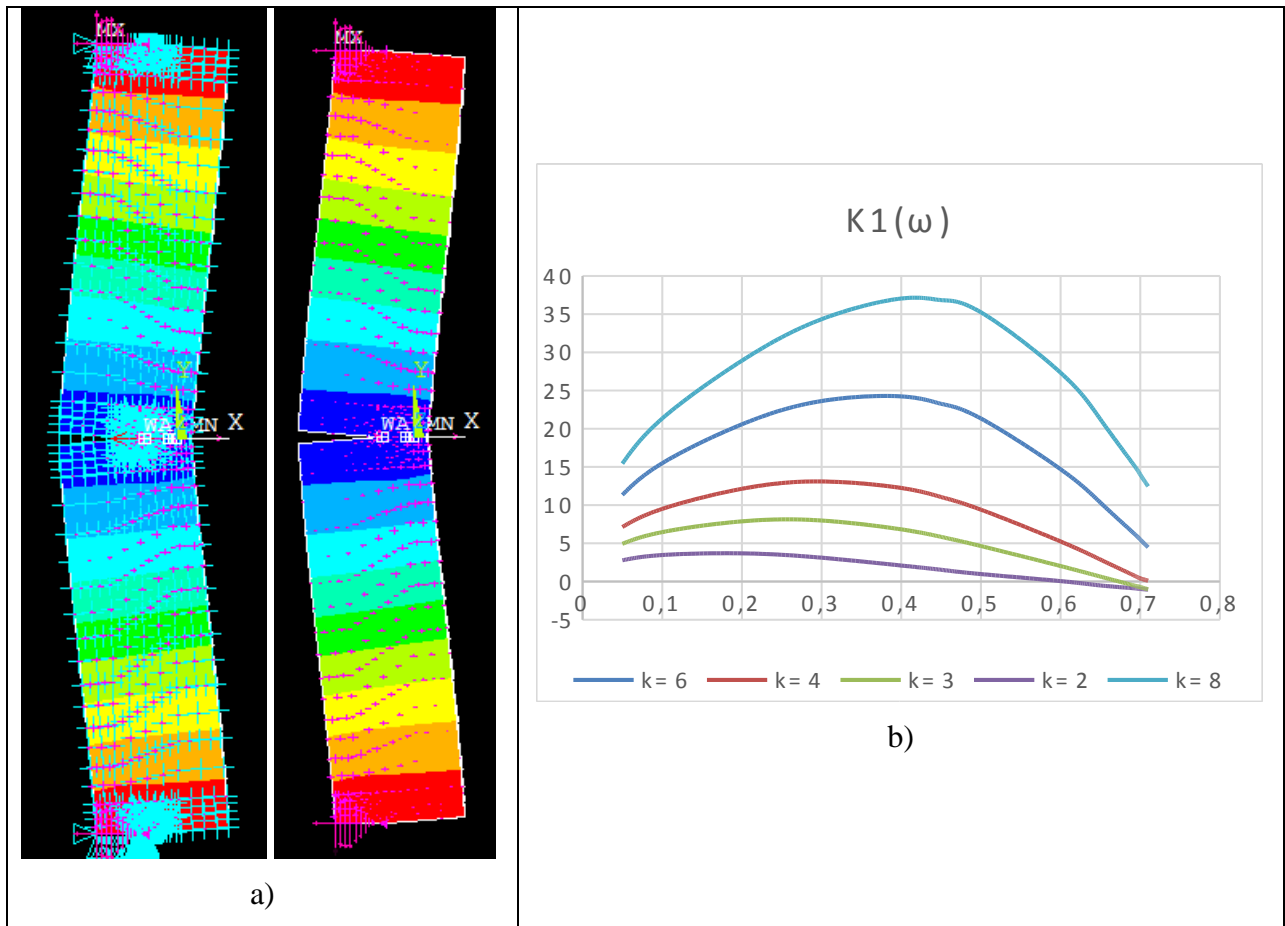


Figure 4. a) Frequency cell for notched beam (ANSYS); b) Plot  $K_I$  vs  $\omega$ .

From the graph  $K_I(\omega)$ , it can be deduced that

- 1 there is such a  $\omega$  max at which the  $K_I$  value is maximum;
- 2 there is such a  $\omega^*$  that  $K_I$  is zero.

The considered problem of constrained bending of a Sodhi beam in the elastic stage has an interesting qualitative feature - the danger of deep notches decreases with increasing depth until it disappears altogether. There is a limit length beyond which the crack cannot grow, the effect of crack closure is due to the occurrence of longitudinal force due to constriction.

### FIXED-ENDS BEAM TEST

In the course of experimental studies in the Sodhi ice basin, he found that the undisturbed zone corresponds to at least one third of the beam thickness ( $h/3$ ). It follows from solution of model elastic problem that crack closure condition ( $K_I=0$ ) for beam length  $k=6$ , corresponds to  $\omega_0=0,75$ ; at  $k=8$ ,  $\omega_0=0,78$ . This means that for relatively long beams, for which the scenario of central and root cracks is true, the compression region turns out to be at least  $h/4$ ...  $h/5$ . From this it can be assumed that perhaps not the whole third of the undisturbed material in D. Sodhi's experiments is in the compression region, some of the material may be in the tensile region adjacent to the crack tip, for which  $K_I < K_{IC}$ .

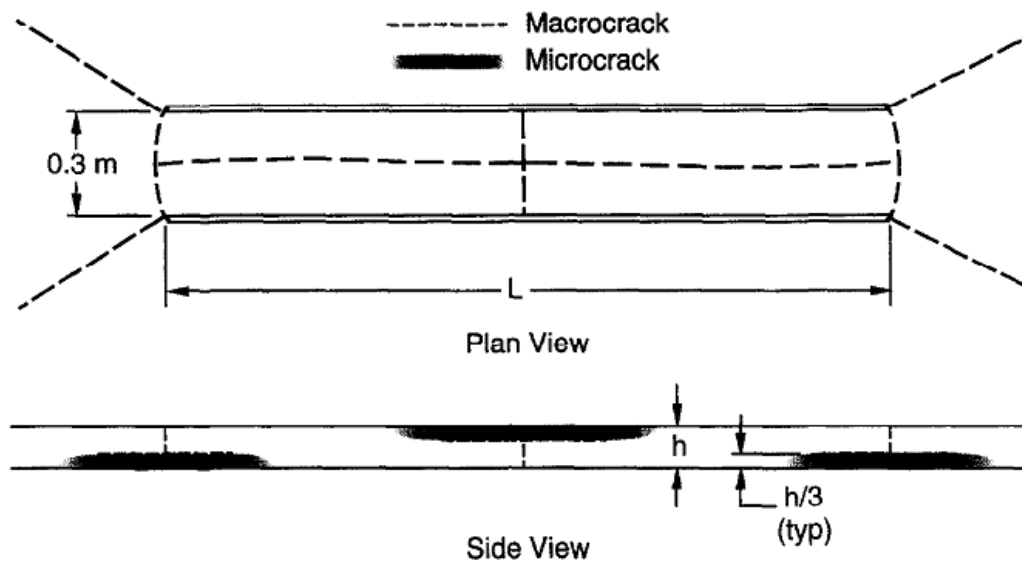


Figure 5. Zones of compression (after Sodhi,1998).

Tests with beams with fixed ends are used to calculate the compressive strength of floating ice. They are also used to verify the results of numerical modelling. During the field tests in Svea in March 2018, a series of bending tests were carried out on a beam with fixed ends (Sodi beam).



Figure 6. Setup for a field test (frames to apply load and to measure deflection and pressure): (a) FEB test (vertical load), and (b) FEB test (horizontal load) with pressure sensors GEOKON (2018-03-08).

The large-scale FEB tests under vertical load were described in previous papers (Karulina, et al., 2016; Sakharov, et. al., 2015). The main features of the FEB tests with horizontal load are the same as in the FEB tests with vertical load, firstly the central crack appeared and then root cracks.

To determine stress distributions, special Geokon sensors were embedded in the beam at key points, based on pressure measurements in the test medium. The sensors consist of two circular stainless steel plates welded around the perimeter and separated by a narrow cavity filled with deaerated oil.

The February test (Figure 6b) with GEOKON sensors was conducted on 8 March 2018 on a floating ice sheet in a fjord near Svea, Svalbard. Ice thickness  $0.6\text{ m}$ , ice temperature  $-8.40^{\circ}\text{C}$ , ice salinity  $5.4\text{ppt}$ . The central crack occurred under a load of  $N_f=32\text{ kN}$ , which allowed the bending strength  $\sigma_f=330\text{kPa}$  to be determined. A prerequisite for the use of test results for the calculation of compressive strength is the failure of the beam in the Sodi scenario: the formation of one vertical central crack and two cracks at the roots of the beam. The ultimate

load (carrying capacity) in the test was  $N_c = 144 \text{ kN}$ . Using Sodi's formula (1998), we can obtain the compressive strength of ice  $\sigma_f = 2 \text{ MPa}$ .

The main purpose of the test (Fig.7) with the GEOKON sensors was to determine the stress distribution during loading. The sensors S1 to S4 have an upper pressure limit of 1 MPa. They were positioned near the line of maximum compression on the cracked beam (non-linear behaviour).

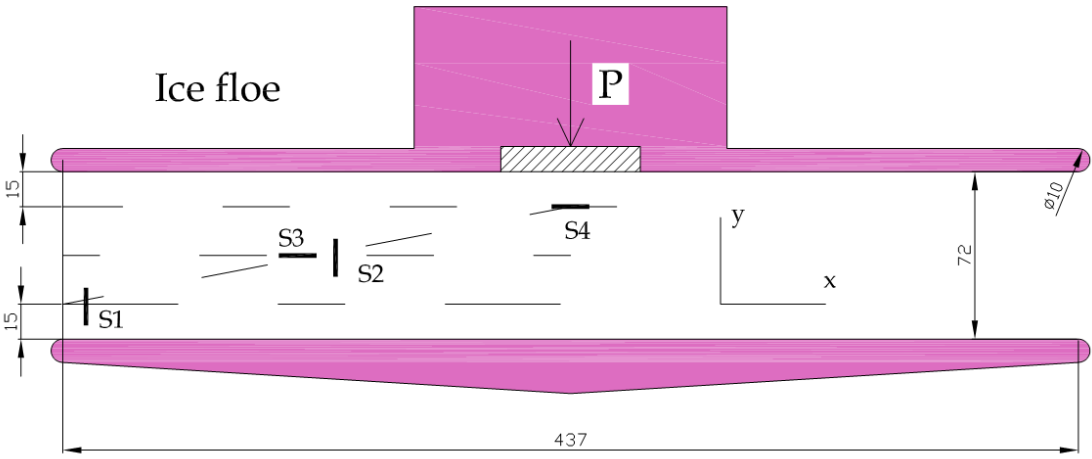


Figure 7. FEB test with GEOKON sensors (S1...S4). All sizes are in cm.

The stress-time curve associated with the Sodi scenario is shown in Figure 8 (a, b). The voltage-time curve according to FEM simulations at the same locations and orientation as the GEOKON sensors is also shown in Fig.8.

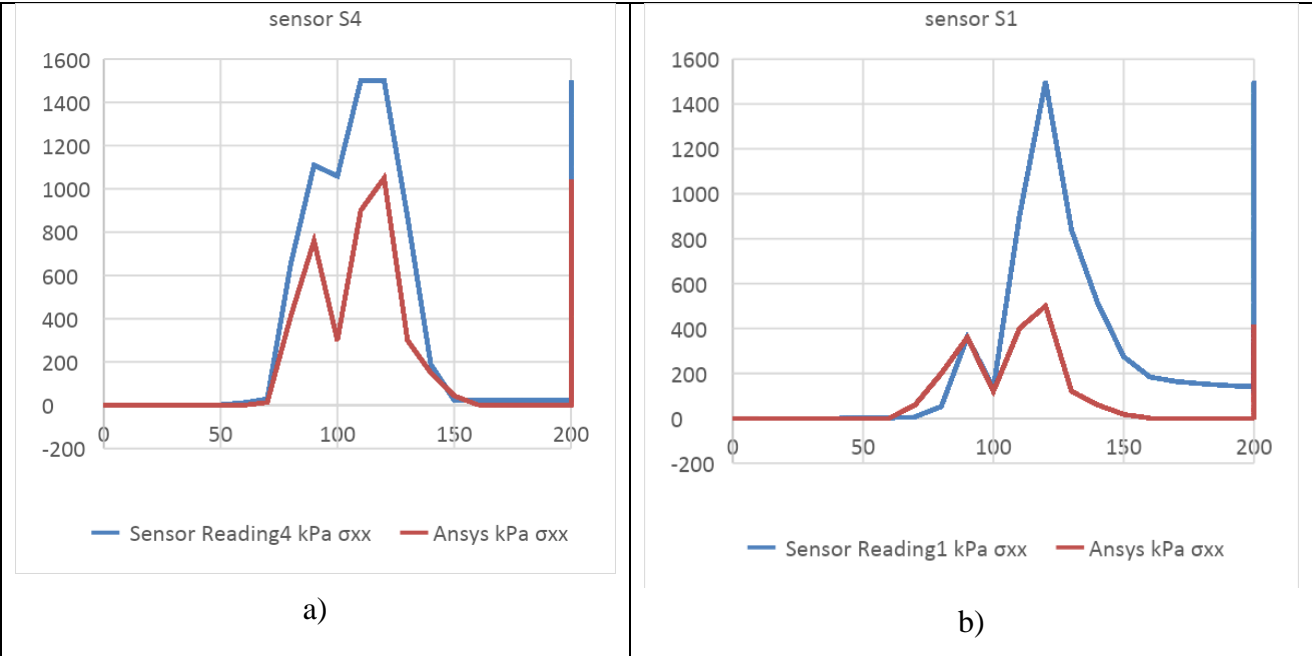


Figure 8. The comparing data reading from sensors S4 (a) and S4(b) and FEM simulation for FEB test with cracks. (Stress kPa vs Time s).

The ANSYS simulations show significantly lower stresses on S1 than the GEOKON sensor measurements. The most reasonable interpretation is that ice exhibits both elastic and inelastic (creep or plasticity) behavior, which must also be considered.

## ACKNOWLEDGEMENTS

The authors wish to acknowledge the support of the Research Council of Norway through the Centre for Sustainable Arctic Marine and Coastal Technology (SAMCoT) and AOCEC project of Int Part program.

## REFERENCES

- Sodhi, D.S. (1998) Vertical penetration of floating ice sheets. *International Journal of Solids Structures*, 35 (31-32): 4275-4294.
- Sanderson T. J. O., *Risks to Offshore Structures*. London, Graham and Trotman. 1988. 253 p.
- Dempsey J.P., Nigam, D., and Cole, D.M. 1988. The flexure and fracture of macrocrystalline S1 type freshwater ice. *Proceedings of the 7<sup>th</sup> International OMAE Conference*, Houston, Texas, Vol. IV, pp 39-46.
- Dempsey J. 1991, The fracture toughness of ice. *Ice-Structure Interaction*, IUTAM-IAHR Symposium, St. John's, Newfoundland, Canada.
- Goldstein, R.V., and Osipenko, N.M. 1983. Fracture mechanics and some questions of ice fracture. *Mechanics and Physics of ice*, Nauka, Moscow, pp.31-62(in Russian).
- Goldstein, R.V., and Osipenko, N.M. 1985. Some mechanism of localized fracture of ice cover under the action of compression. *Proceedings of the 8<sup>th</sup> International POAC Conference*, Narssarsuaq, Greenland, Vol.3, pp. 1170-1188.
- Slepyan, L. Dempsey, J., and Shekhtman, I., 1995. *Crack Closure and Related Problems*. Ice Mechanics
- J. R. Rice and N. Levy, 1972. "The Part-Through Surface Crack in an Elastic Plate", *Journal of Applied Mechanics*, 39, pp. 185-194.
- Tada K, Oka M, Tangoku A, Hayashi H, Oga A, Sasaki K. 2000. Gains of 8q23-qter and 20q and loss of 11q22-qter in esophageal squamous cell carcinoma associated with lymph node metastasis.
- Karulina, M., Marchenko, A., Sakharov, A., Karulin, E., Chistyakov, P., 2016. Experimental Studies of Fracture Mechanics for Various Ice Types. . *Proc. of the 23rd IAHR Symposium on Ice*, Ann Arbor, Michigan, paper 4869357.
- Karulina, M., Marchenko, A., Sakharov, A., Karulin, E., Chistyakov, P., 2018. Experimental studies of Sea and Model Ice Fracture Mechanics. In book *The Ocean in Motion*, M.G.Velarde, R.Yu.Tarakanov, A.V.Marchenko (Editors), Springer, 591-610
- Marchenko, A., Karulin, E., Chistyakov, P., Sodhi, S., Karulina, M., Sakharov, A., 2014. Three dimensional fracture effects in tests with cantilever and fixed ends beams. *Proc. of the 22th IAHR Symposium on Ice*, Singapore, paper 1178
- Sakharov, A., Karulin, E., Marchenko, A., Karulina, M., Sodhi, D., Chistyakov, P., 2015. Failure envelope of the brittle strength of ice in the fixed-ends beam test (two scenarios). *POAC15-00230*, Trondheim, Norway, 8 pp